

Storm severity nowcasting by real-time return period imaging

M. Reyniers¹, L. Delobbe¹, P. Dierickx², M. Thunus², C. Tricot¹

¹Royal Meteorological Institute of Belgium, Ringlaan 3,
1180 Brussels, Belgium, e-mail: maarten.reyniers@meteo.be

²Hydrological service of the Walloon administration (Service Public
de Wallonie, SPW), Boulevard du Nord 8, 5000 Namur, Belgium

(Dated: 30 June 2010)

Abstract

We report on the implementation of a real-time product at the Royal Meteorological Institute of Belgium (RMI) that combines radar data with Intensity-Duration-Frequency (IDF) curves, in order to get an estimate of the return period of an ongoing event, as a measure of the storm severity. The product was developed on request of the hydrological service of the Walloon Region (southern part of Belgium). Experience in this hydrological service has shown that the hydrological model that is used for issuing flood warnings over the Walloon river catchments, Hydromax, performs well in widespread, large-scale precipitation, but that it largely fails in extreme local rainfalls causing flash floods. Therefore, a specialised product allowing fast reaction is needed in these situations. For this purpose, precipitation accumulation images with different durations from two C-band radars are compared in real-time with IDF curves recently determined by the RMI. We will show that, despite the large uncertainties both in the rainfall accumulations based on radar data and in the IDF curves, the product is a very useful nowcasting tool in the case of extreme events.

1. Introduction: need for a specialised product

Hydrological services are one of the most important end-users of radar imagery. Nowadays radar images serve as an indispensable complement to the information provided by the “classical” rain and stage gauges in hydrological applications. Sophisticated hydrological models are able to ingest radar images to produce predictions of river stages and alerts for possible floods. The hydrological service of the Walloon Region uses a real-time application for riverflow forecasting “Hydromax” which is developed by CESAME (Université Catholique de Louvain, Belgium) and is operational at the SPW (Service Public de Wallonie) for the management of flood alarms and the on-line information of the rescue services in the Walloon river catchments. The system ingests the data from the telemetric rain and stage gauges in near-real time (for more details, see Bastin et al., 2009). One of the end-products of the system is an on-line map showing zones in which floods can possibly develop in the next hours. In the near future, the current version of Hydromax will be complemented by a version that also ingests radar data.

Although the telemetric network of the SPW is very dense (1 gauge per 193 km²), a rain gauge network is never able to capture the same spatial detail of precipitating areas as a weather radar. On the other hand, the accuracy of the point measurements provided by rain gauges is much higher than the accuracy of the radar value at the gauge location. A quantitatively reliable precipitation map can thus be obtained by combining (merging) both rain gauges (accuracy) and radar images (spatial detail). At the RMI, a project was initiated in Nov. 2007 together with the SPW to search for the most accurate technique to merge gauges and radar information. The results of this study are published in an international magazine (Goudenhoofd & Delobbe, 2009), and they will ultimately lead to an operational radar-gauge correction product that will be supplied to the SPW.

In widespread large-scale precipitation events, the spatial variance is low, and the ingestion of radar images will not much contribute to the performance of the hydrological model. However, in the case of heavy local precipitation induced by convective weather (e.g. in the form of supercells), it is likely that only radar images capture such an event adequately. But even with the ingestion of radar data into the hydrological model, the handling of such events is problematic: (1) hydrological models are not always tuned for such events since these situations are rare, and (2) waiting for the model output can take some time, while action has to be taken as quick as possible.

In a hydrological context, the most dangerous situations are those in which convective cells are stationary. Such stationary cells can develop for example if the intrinsic cell movement is opposite to the wind direction, making the net movement to be zero. An example of such a situation is shown in **Fig. 1**. Another type of situation very threatening in a hydrological context, is shown in **Fig. 2**, in which a line of precipitation moves parallel to its orientation. We will use these two particular situations throughout the paper to illustrate the new product. These situations are especially dangerous, since large amounts of precipitation are collected in the same basin. Unfortunately, such conditions are difficult to recognise on a single radar image, and can only be discovered by studying cumulative images with accumulations made on several time periods (e.g. 10 min, 20 min, 1/2 hour, 1 hour, 2 hours, ...). Moreover, an accumulative value can only be confirmed to be “exceptional” by comparing it to its return period. These return periods are given in so-called IDF curves (intensity-duration-frequency), giving the return period (frequency) of a certain amount of precipitation (intensity) during a certain time span (duration). In

the product discussed in this paper, we condense all this information into one single image, expressing the “severity” of a situation in terms of the return period of the unfolding event. First, a number of real-time accumulation maps will be made for several durations, and then every accumulation map is converted into a return-period map showing the return period for every pixel of that accumulated value. For every pixel on the final map, the maximum is taken over all the return period maps. In this way, the users have a direct indication of the severity of an ongoing event, without the need of running any hydrological model.

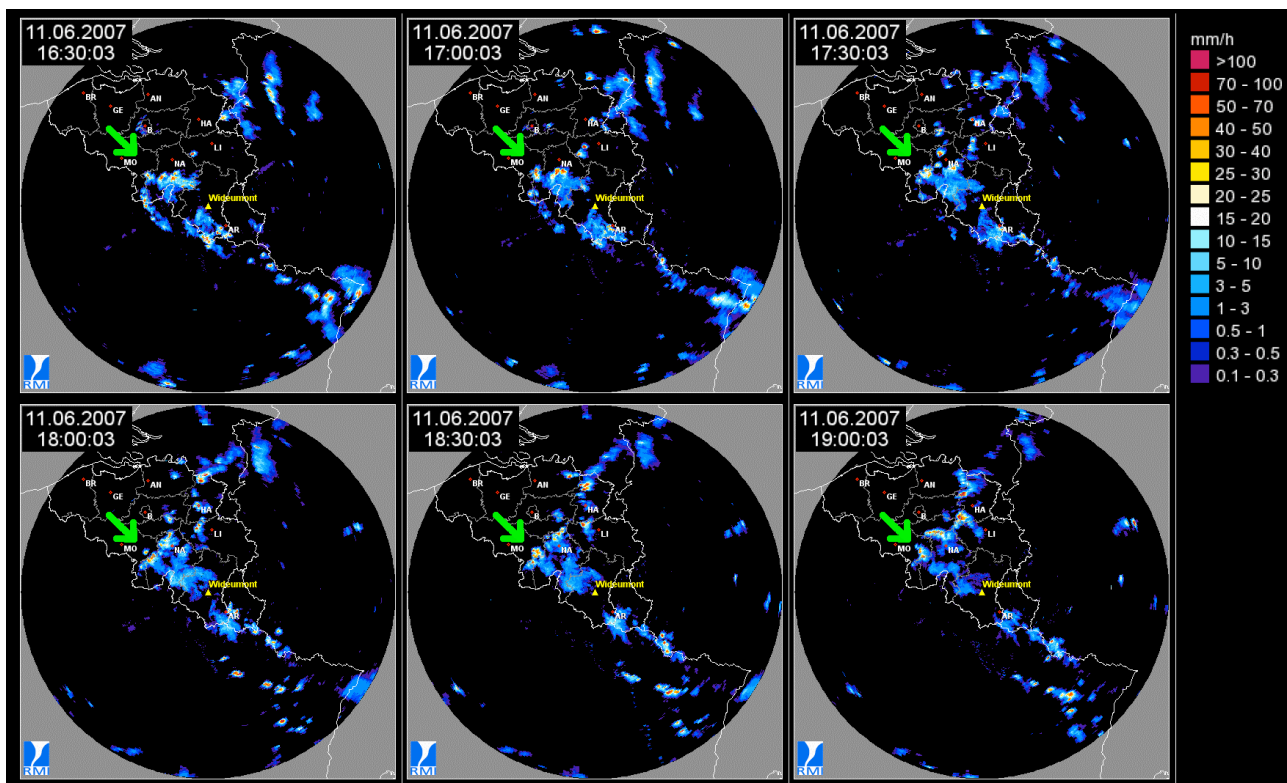


Figure 1: An example of an event with stationary cells (Wideumont radar, 11 June 2007, 16h30-19h00 UT). The green arrow indicates such a cell.

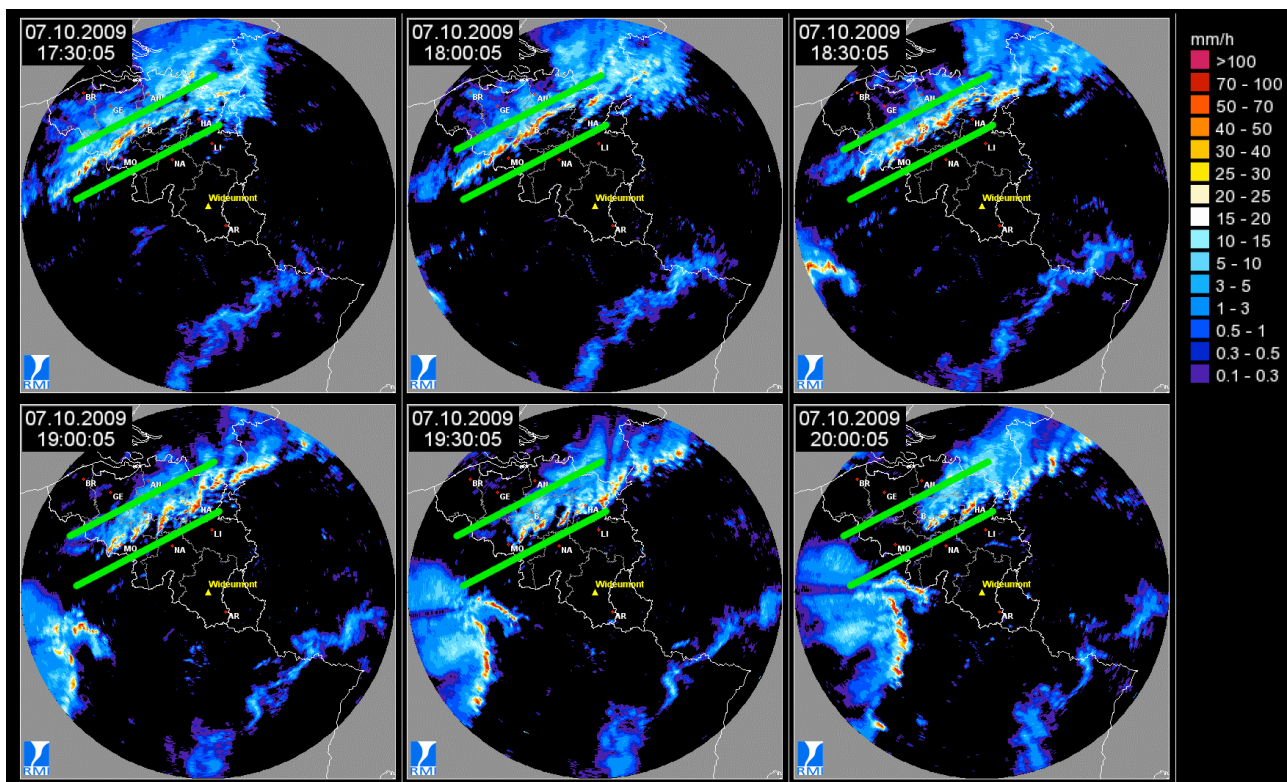


Figure 2: An example of a line of precipitation moving parallel to its orientation, producing also very high accumulations (Wideumont radar, 07 October 2009, 17h30-20h00 UT). The region between the two green lines suffered from very severe rainfall during several hours.

2. Input: IDF maps and radar data

IDF curves (Intensity-Duration-Frequency) give the relation between rainfall intensity I (in mm or mm h^{-1}), the duration (D) of the accumulation and the return period (T). IDF maps for Belgium were recently determined by the RMI (Mohyont and Demarée, 2006). Examples of these maps are given in **Fig. 3**. The RMI has gauge data of roughly 375 stations. 345 of these stations are part of the climatological network, reporting daily accumulation values. Most of these stations started in 1951. The remaining 30 stations have an update frequency of 10 minutes, and provide data back to 1967. In order to achieve a homogeneous data set to calculate the IDF curves, only those stations were selected with a time series of minimum 25 years, which started before 1968 and ended not sooner than 1993, and in which not more than 10% of the values were missing. With these criteria, the final number of daily stations used in the project decreased to 184, while the number of 10-min stations decreased to 22. IDF maps were generated by kriging with a resolution of $7 \times 7 \text{ km}^2$.

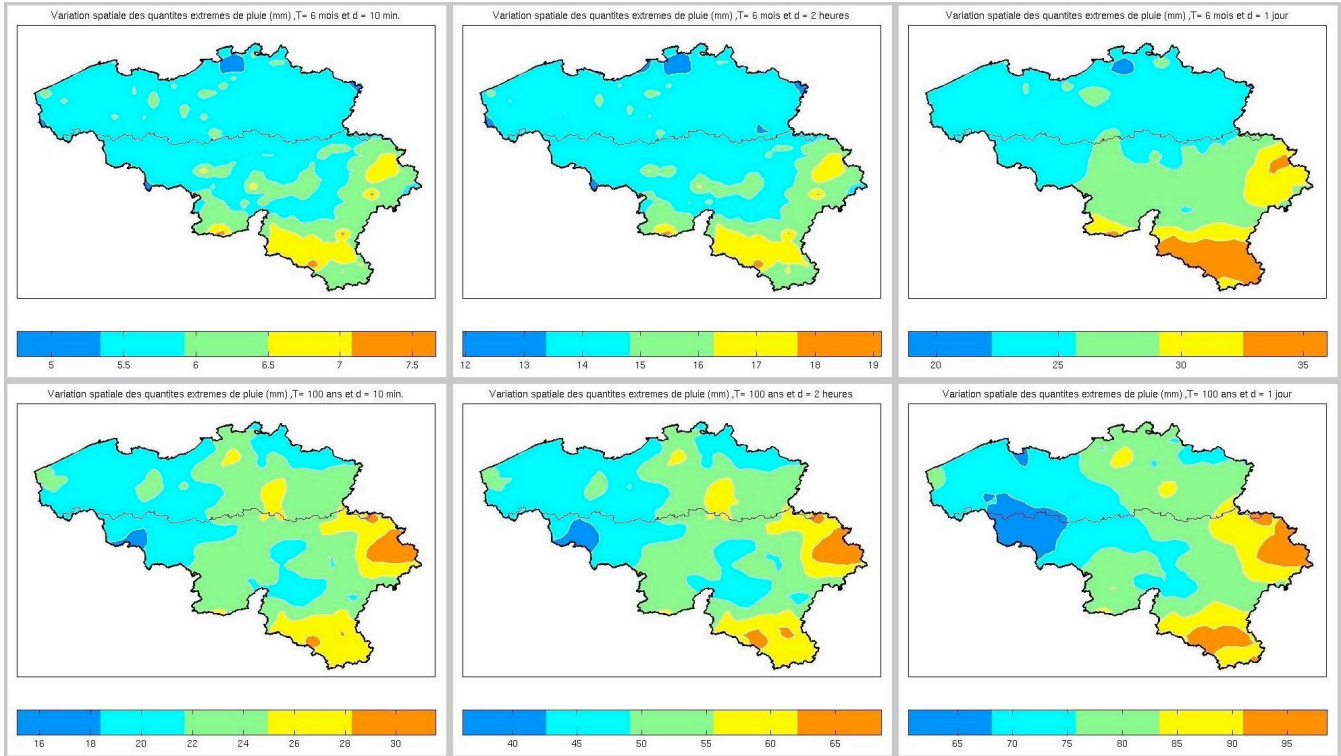


Figure 3: IDF map examples. Shown here are the IDF maps (in mm) for a return period of 6 months (upper row) and a return period of 100 years (lower row). For each return period, durations of 10 minutes (left column), 2 hours (middle column) and 1 day (right column) are shown. Note that the scale is different for each image.

The storm severity product was implemented for two radars. The first one is the weather radar of Wideumont, in the south of Belgium, which is owned and operated by the RMI. It was installed in 2001 and has a maximum range of 240 km (see e.g. Delobbe and Holleman, 2006, for more technical details of this radar). The second one is the Avesnois radar, installed by Météo-France in 2005, with a financial participation of the Walloon Region. The maximum range is 256 km. Both radars are C-band radars and generate a pseudo-CAPPI every 5 minutes, which is used here as input for the product. The relation $Z = aR^b$ with $a = 200$ and $b = 1.6$ is applied to convert radar reflectivities into rainrates.

3. Method

The preparatory work consisted of the interpolation of the IDF maps to the radar grid of the accumulation images. In the operational context, the following steps are executed every time a new radar image (pseudo-CAPPI) becomes available:

- Calculate the precipitation accumulations for different time windows in a computational cheap way. The accumulations are real-time, so the time windows for these accumulations are “running” (conventional accumulations are calculated for a fixed time span, i.e. between x and y h UT);
- Combination of the calculated accumulations with the IDF grid to real-time “return-period images”;
- Combination of the “return-period images” to one single return-period image as the final output of the product. For every pixel on the map, the maximum of the return periods for that pixel is taken. This maximum is then a measure for the “severity” of the event as it develops.

The method is schematically illustrated in **Fig. 4**. The real-time accumulations are calculated for the following eight durations: 10 min, 20 min, 30 min, 1 h, 2 h, 6 h, 12 h and 24 h. Every time a new radar image arrives (in normal operation, every five minutes for both radars), each accumulation is updated using this latest image. To minimize the CPU time, the algorithm “recycles” the previous accumulation calculation, and evaluates which radar image has to be added or subtracted from the different accumulation durations. The accumulations of the situation depicted in Fig. 1 are shown in **Fig. 5**.

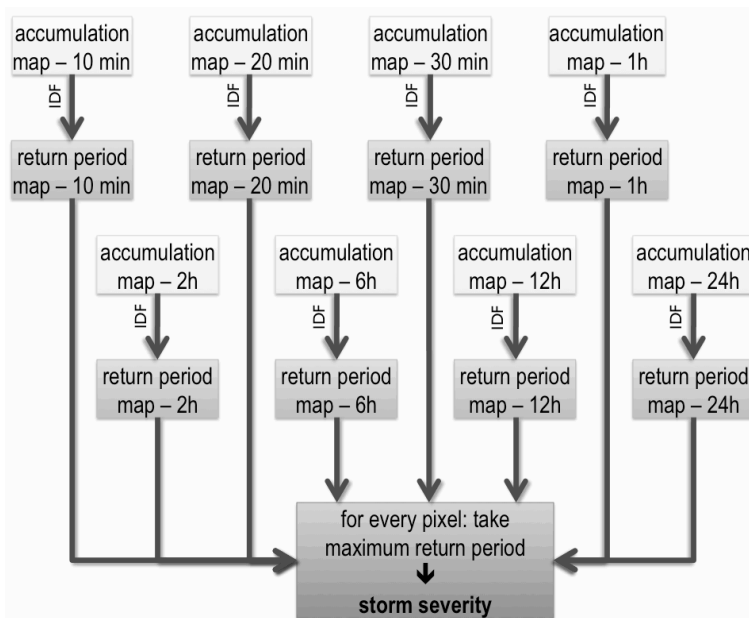


Figure 4: Scheme of the dataflow of the storm severity product. This scheme is executed each time a new radar image becomes available.

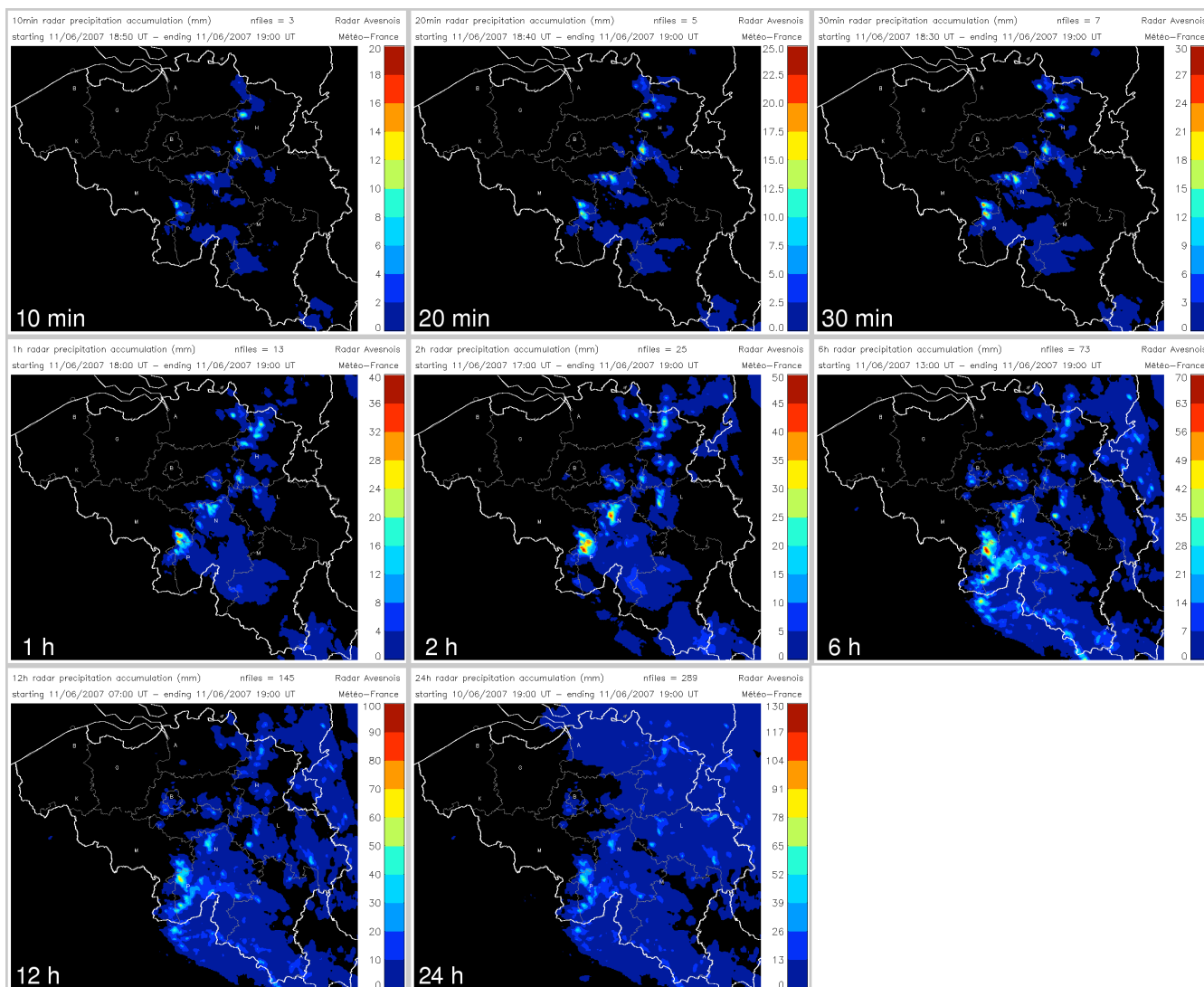


Figure 5: Accumulations for the same situation that was shown in Fig. 1 (radar de l’Avesnois). The following accumulations are calculated: top row 10 min, 20 min, 30 min; middle row 1 h, 2 h, 6 h; bottom row 12 h and 24 h. The end time of all these accumulations is 19h00 UT. Note that the scale of the images increases for longer accumulation durations.

4. Results: two case studies

4.1. Stationary cells 11/06/2007

In **Fig. 6** an example of the final product is shown. It is the same case that was shown in Figs. 1 and 5. The map on the left is the main map of the product. It shows the maximum return period of the rainfall for the past durations mentioned above, and relies for this on the real-time accumulations discussed in the previous section and calculated following the scheme in Fig. 4. Since the IDF curves were only calculated for the Belgian territory, the return period map is limited to Belgium as well. The map on the right specifies for which duration this maximum return period is reached, so it expresses at which timescale the most severe rainfall occurred. From Fig. 6, it is clear that the real-time return period product is a very powerful filter to immediately detect the locations that are strongly affected by heavy rain in the past 24 hours. Indeed, the area that was marked in Fig. 1 with a green arrow as the location of a stationary cell producing very large local rainfalls, is characterised by a very long return period in Fig. 6.

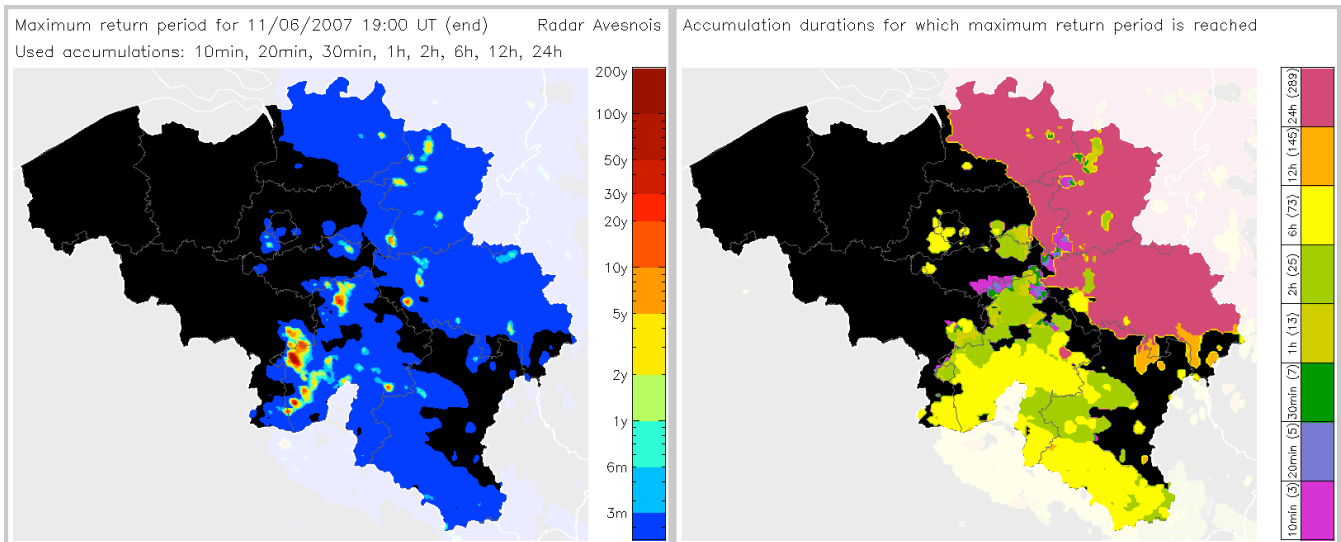


Figure 6: Result of the storm severity product for the same situation that was shown in Fig. 1 (Avesnois radar, 11 June 2007, 19h00 UT). The numbers between brackets in the legend of the map on the right denote the number of radar files that were used for that particular accumulation duration.

4.2. Severe precipitation 07/10/2009

A second example of the product is shown in **Fig. 7**, which is the episode shown in Fig. 2. During this episode, several complexes crossed Belgium. The complex that entered Belgium around 17h00 UT in the west, was peculiar in the sense that its displacement was parallel to its orientation, causing very high local accumulations and even flash floods in some regions. The region marked in red on Fig. 7 clearly indicates the passage of this complex through Belgium.

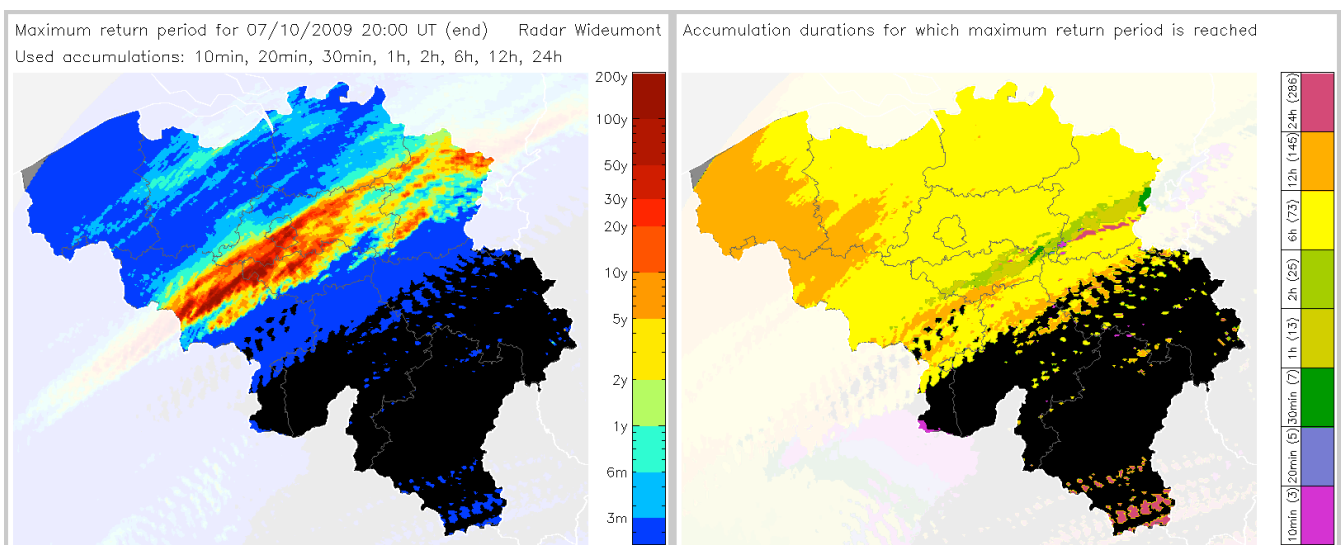


Figure 7: Result of the storm severity product for the situation with a line of precipitation moving parallel to its orientation, shown in Fig. 2 (Wideumont radar, 07 October 2009, 20h00 UT). Very high accumulations were recorded for a region extending from the west to the northeast.

5. Limitations of the product

The real-time return period map can be used to quickly estimate the “severeness” of a given event. However, the end-users should certainly be aware of the limitations of the product. For example, it is well known that for high radar reflectivities, the calculation of a reliable rainrate is hampered by the contamination of hail. Therefore the highest return periods (say >30y) are the least reliable, and should only be used qualitatively. In general, the return periods produced by the product should never be used as real and validated climatological values, but only as indicative values.

Another source of error is the fact that the real-time accumulated rainrates are calculated with radar data, while the IDF curves are based on historical gauge data. A possible solution to decrease this uncertainty could be the merging of the radar data with real-time gauge data. Our group (Goudenhoofdt & Delobbe, 2009) recently studied different methods to merge radar data and rain gauge data. However, since the storm severity product must be available as soon as possible after the receipt of a new radar file, this merging cannot be applied here: the gauges in our network do not have the same update frequency as the radar images. Moreover, the product also focuses on events with very local rainfall; in these situations the radar-gauge merging is less efficient due to the high spatial variation of the rainfield that cannot be accurately captured by a gauge network, even if it is very dense.

In principle, the accuracy of the product could be considerably improved if also the IDF curves were determined based on radar data itself, instead of on gauge data. Weather radars are operationally used in many meteorological services for more than a decade now, so attempts to derive climatological information of rainfall based on radar data are more and more appearing (e.g. Overeem, 2009). Our radar is operational since 2001, so for the moment our archive might still be on the short side to derive radar-based IDF information, but in the future this will be certainly feasible.

Other notable artefacts that can show up in the final product, are strong contaminations by the bright band, and permanent or anaprop induced ground echoes. These effects are well-known artefacts frequently seen in radar accumulation images, so it is expected that the same effects are seen in the real-time return period images as well. Our group is planning to introduce an operational VPR correction (Vertical Profile of Reflectivity) that should eliminate the bright band effect efficiently (Vazquez Alvarez et al., 2010). Note, however, that in Belgium the bright band effect is a typical phenomenon of the cooler seasons, while the product is designed to be used in the case of convective events, which mainly occur in summer.

6. Conclusions

We have developed a new product at the RMI for the real-time detection of heavy local rainfall. The product generates in real time a map that indicates the return period of the ongoing event. Due to the large uncertainties in radar-based rainfall accumulations and in the IDF curves on which it is based, it offers only a qualitative view on the real-time return periods. Nevertheless, the product is a valuable nowcasting tool for the real-time evaluation of the severity of an ongoing event, and it allows fast reaction by the hydrological service in case of potential flash floods, without running a time-consuming hydrological model.

Acknowledgements

We are indebted to Météo-France for providing us the data of the Avesnois radar. Christophe Ferauge and Geert De Sadelaer are thanked for the technical support in the development.

References

- Bastin G., Moens L., Dierickx P., 2009: On-line river flow forecasting with ‘Hydromax’: successes and challenges after twelve years of experience. *Proceedings of the 15th IFAC Symposium on System Identification*, Saint-Malo, France, July 6-8, 2009
- Delobbe L., Holleman I., 2006: Uncertainties in radar echo top heights used for hail detection. *Meteorological Applications*, **13**, 361–374
- Goudenhoofdt E., Delobbe L., 2009: Evaluation of radar-gauge merging methods for quantitative precipitation estimates. *Hydrology and Earth System Sciences*, **13**, 195–203
- Mohyont B., Demarée G.R., 2006: final report IDF curves for the Walloon Region, Ministère Wallon de l’Equipement et des Transports, Cahier spécial des charges MS/212/2003/08, available on <http://voies-hydrauliques.wallonie.be/>
- Overeem A., 2009: Climatology of extreme rainfall from rain gauges and weather radar. *PhD thesis*, Wageningen University, the Netherlands
- Vazquez Alvarez M., Goudenhoofdt E., Delobbe L., 2010: Implementation and evaluation of VPR correction methods based on multiple volume scans. *This volume*